Effect of selenium deficiency on the thermoelectric properties of *n*-type In_4Se_{3-x} compounds

G. H. Zhu,[1] Y. C. Lan,[1] H. Wang,[1] G. Joshi,[1] Q. Hao,[2] G. Chen,[2,*] and Z. F. Ren[1,†]

[1]*Department of Physics, Boston College, Chestnut Hill, Massachusetts 02467, USA*

[2]*Department of Mechanical Engineering, Massachusetts Institute of Technology, Cambridge, Massachusetts 02139, USA*

(Received 22 November 2010; published 4 March 2011)

Thermoelectric properties of dense bulk polycrystalline In_4Se_{3-x} ($x = 0$, 0.25, 0.5, 0.65, and 0.8) compounds are investigated. A peak dimensionless thermoelectric figure of merit (ZT) of about 1 is achieved for $x = 0.65$ and 0.8. The peak ZT is about 50% higher than the previously reported highest value for polycrystalline In_4Se_{3-x} compounds. Our In_4Se_{3-x} samples were prepared by ball milling and hot pressing. We show that it is possible to effectively control the electrical conductivity and thermal conductivity by controlling selenium (Se) deficiency x. The ZT enhancement is mainly attributed to the thermal conductivity reduction due to the increased phonon scattering by Se deficiency, defects, and nanoscale inclusions in the ball-milled and hot-pressed dense bulk In_4Se_{3-x} samples.

DOI: 10.1103/PhysRevB.83.115201 PACS number(s): 72.20.Pa

I. INTRODUCTION

Solid-state energy conversion between heat and electricity based on thermoelectric effects has attracted extensive interest for many decades.[1] Thermoelectric devices can be used for environmentally friendly refrigeration and power generation. The efficiency of thermoelectric devices is determined by a dimensionless thermoelectric figure of merit $ZT = (S^2\sigma/\kappa)T$, where S, σ, κ, and T are the Seebeck coefficient, electrical conductivity, thermal conductivity, and absolute temperature, respectively.[1] Considerable effort has been made to improve the ZT values of the existing thermoelectric materials or to discover new high ZT materials. Recently, a noticeably high ZT was achieved in the b-c plane of $In_4Se_{2.35}$ single crystals.[2] In_4Se_3 crystallizes in a layered structure with weak van der Waals bonding between the layers along the a axis and strong covalent bonding within the layer (b-c plane).[2,3] Due to charge-density wave (CDW) and Peierls distortion, the thermal conductivity in the b-c plane of the bulk single crystal $In_4Se_{2.35}$ is greatly reduced.[2] However, $In_4Se_{2.35}$ single crystals prepared by the unidirectional crystal-growth method, such as Bridgeman technology, have remarkable anisotropy. Although $In_4Se_{2.35}$ is reported to have a ZT value of 1.48 at 432 °C in the b-c plane, the ZT value in the a-b plane is much lower, around 0.5 at 432 °C.[2] Although polycrystalline In_4Se_{3-x} compounds do not have an anisotropy problem, the highest reported ZT is only about 0.6,[4,5] which is not good enough for practical applications. In the past decade, numerous experimental and theoretical studies have shown that nanocomposite and nanostucturing approaches are effective in improving ZT.[6–11] In nanostructured systems, the enhanced ZT comes from a significant reduction in phonon thermal conductivity. Nanoscale grains and inclusions are believed to strongly scatter phonons, which have relatively longer mean free paths than those of the electrons.[12–14] We note that In_4Se_3 single crystals have relatively high electrical resistivity, and the thermal conductivity mainly comes from the lattice thermal conductivity. Thus we applied the ball milling and hot-pressing approach[7–11] to the In_4Se_{3-x} system, expecting to observe reduced lattice thermal conductivity due to the enhanced phonon scattering by nanograins and/or nanostructures in hot-pressed samples. Furthermore, different Se deficiency x in In_4Se_{3-x} samples were prepared so as to optimize the thermoelectric properties.

II. EXPERIMENT

In our work, different amounts of indium (In) and selenium (Se) elements were mixed together and pulverized into nanopowders by ball milling. All weighing and loading of the materials were operated inside a glove box filled with argon gas. The nanopowders were hot pressed into discs by a quick direct-current-induced hot-pressing process at 540 °C. X-ray diffraction (XRD, Bruker-AXS, D8), scanning electron microscopy (SEM, JEOL-6340F), and high-resolution transmission electron microscopy (HRTEM, JEOL-2010F) were used to characterize the nanopowders and hot-pressed bulk samples. The electrical conductivity and Seebeck coefficient were measured simultaneously on the same bar samples of about $2 \times 2 \times 12$ mm in a multiprobe transport system (Ulvac ZEM-3). The thermal diffusivity (α) was measured using a laser flash system (Netzsch LFA 457) and the heat capacity (C_p) was measured by a commercial differential scanning calorimeter (DSC 200 F3). The density of the hot-pressed samples was measured using an Archimedes kit. The density of our hot-pressed In_4Se_{3-x} ($x = 0$–0.8) samples is ~5.93–6.03 g cm^{-3}, which is very close to the theoretical value. The thermal conductivity κ is obtained as the product of thermal diffusivity (α), sample density (ρ), and heat capacity, $k = \alpha_p C_p$.

III. DISCUSSION AND CONCLUSIONS

Figure 1 shows the XRD pattern of $In_4Se_{2.35}$ bulk samples after hot pressing. The XRD pattern confirms that the major phase of our samples is the In_4Se_3 phase. Since In_4Se_{3-x} is thermodynamically unstable,[15] a weak peaks of indium impurity phase was also detected in some of the In_4Se_{3-x} samples.

Figure 2 shows the transport properties of In_4Se_{3-x} samples with different Se deficiency concentrations ($x = 0$, 0.25, 0.5, 0.65, and 0.8). The electrical resistivity ρ dependence of temperature as shown in Fig. 2(a) and the dependence of Se deficiency x, shown as the inset, indicate that the resistivity first decreases with increasing Se deficiency concentration up to

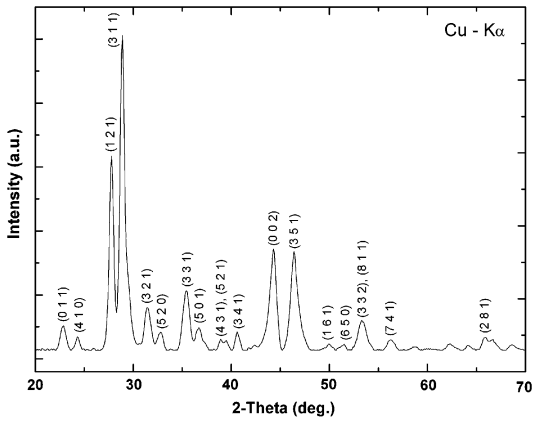

FIG. 1. XRD pattern of dense bulk samples $In_4Se_{2.35}$ after hot pressing.

$x = 0.5$, then increases with x. With increasing Se deficiency x from 0 to 0.8, In_4Se_{3-x} samples change conducting behaviors: In_4Se_3 and $In_4Se_{2.2}$ are semiconductors whereas $In_4Se_{2.5}$ shows semimetallic behaviors, especially at around room temperature, with both hole and electron carriers, which results in a relatively lower electrical resistivity of $1.7 \times 10^{-4}\Omega$ m at room temperature. The effective carrier concentration n of $In_4Se_{2.5}$, measured by using the van der Pauw method,[16] is 1.68×10^{18} cm^{-3} at 25 °C, almost two orders of magnitude higher than 4.02×10^{16} cm^{-3} (In_4Se_3) and 4.13×10^{16} cm^{-3} ($In_4Se_{2.2}$). The mobility of In_4Se_{3-x} samples varies from 29.1 cm^2 V^{-1} S^{-1} ($In_4Se_{2.5}$) to 189 cm^2 V^{-1} S^{-1} (In_4Se_3), which is lower than the reported value.[4] The relatively low mobility in our In_4Se_{3-x} samples is mainly due to the increased scattering of the charge carriers by the increased number of grain boundaries and defects in our ball-milled and hot-pressed samples.

Large negative Seebeck coefficient values are observed in $In_4Se_{2.2}$, $In_4Se_{2.35}$, and In_4Se_3 samples [Fig. 2(b)]. The semiconducting $In_4Se_{2.2}$ sample shows a maximum Seebeck coefficient of about -560μV K^{-1} at room temperature, whereas semimetallic $In_4Se_{2.5}$ sample shows the lowest Seebeck coefficient of -26μV K^{-1} at room temperature due to the existence of both types of carriers. The thermoelectric power factor ($S^2\sigma$) is shown in Fig. 2(c). Because of the low electrical transport properties, $S^2\sigma$ values are small for all In_4Se_{3-x} samples.

Figures 2(d) and 2(f) show the temperature dependence of the thermal conductivity κ and dimensionless figure of

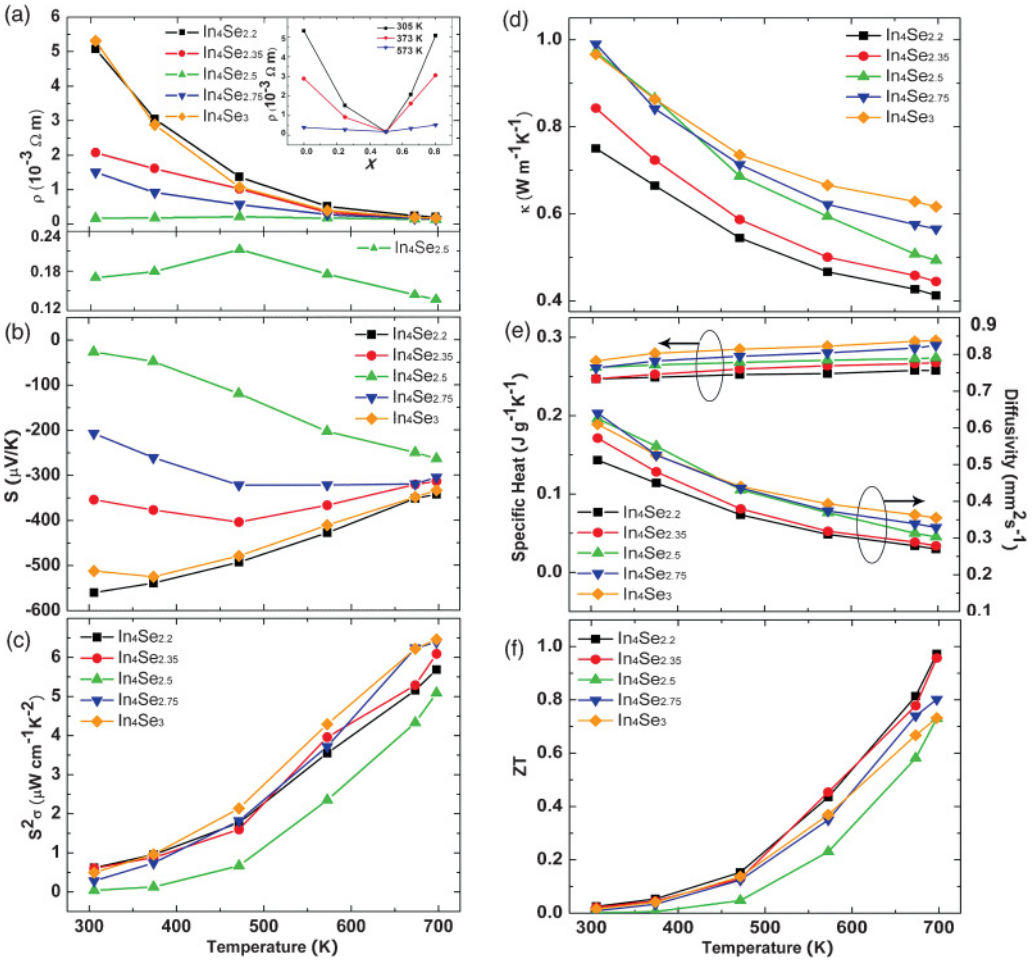

FIG. 2. (Color online) Temperature-dependent electrical resistivity (a), Seebeck coefficient (b), power factor (c), thermal conductivity (d), specific heat C_p and diffusivity (e), and ZT (f) of hot-pressed dense bulk samples In_4Se_{3-x}. The inset in (a) shows the electrical resistivity dependence of Se deficiency.

merit *ZT*. As shown in Fig. 2(d), the thermal conductivity κ decreases from 0.75W m^{-1} K^{-1} to 0.41W m^{-1} K^{-1} at 425 °C with increasing temperature for $In_4Se_{2.2}$, which has the lowest thermal conductivity among all samples, about 40% lower than the reported value in the polycrystalline In_4Se_{3-x} compounds.[4] The low thermal conductivity in our In_4Se_{3-x} samples should be attributed to the defect-induced phonon scattering by the Se deficiency sites and enhanced phonon scattering due to the higher grain-boundary density. Figure 2(e) shows the thermal diffusivity and specific-heat capacity values of In_4Se_{3-x} samples. Very low diffusivity values are observed in all In_4Se_{3-x} samples and the diffusivity decreases with increasing Se deficiency in the high-temperature region, indicating strong phonon scattering by Se vacant sites. *ZT* [Fig. 2(f)] increases with temperature and reaches the maximum value at 425 °C. Owing to the significantly reduced thermal conductivity, the hot-pressed In_4Se_{3-x} samples exhibit peak *ZT* values of 0.97 and 0.96 at 425 °C for $In_4Se_{2.2}$ and $In_4Se_{2.35}$ samples, respectively.

In order to understand the mechanism of the thermal conductivity reduction and *ZT* enhancement in the hot-pressed In_4Se_{3-x} samples, preliminary TEM studies were carried out. The TEM specimens were prepared by both focused ion beam (FIB) using the standard H-bar method and mechanical polishing down to several microns using tripod polishing technique, then Ar^+ ion milling using Gatan precision ion polishing system (PIPS). Unfortunately it turned out that the sample preparation is very challenging; the specimens were very easily contaminated. It seems that the contamination was caused by the materials decomposition and recrystallization on the specimen surface during the FIB and ion-milling process. Figure 3(a) shows a typical TEM image of the ion-milled TEM specimens for $In_4Se_{2.2}$ from which we can clearly see that the average grain size is about 400–700 nm, due to the grain growth during the hot-pressing process. Although the grain size is much smaller than the conventional polycrystalline compounds, they are still too big to effectively scatter phonons and cannot be the reason to explain the low thermal conductivity in Fig. 2(d). In order to study the microstructures of the grains by HRTEM, a clean specimen was carefully mechanically polished to electron transparency without using Ar^+ ion milling to prevent contamination. The TEM specimen prepared in such a way is clean without any contamination, but the area which is thin enough for HRTEM is rather small. HRTEM of the $In_4Se_{2.2}$ specimen [Fig. 3(b)] shows that there are some nanoscale features of sizes up to 10 nm inside the grains. The energy dispersive x-ray spectroscopy (EDS) result shows that the nanoscale inclusions have the same composition with the nearby matrix within EDS experimental error (±1 atm %). Moreover, we also noticed that there are many dislocations and point defects in our hot-pressed samples. In order to investigate the dislocations in the specimens, the fast-Fourier-transform (FFT) of HRTEM images are generated using the DigitalMicrograph software (Gatan Inc., PA). A series of inverse fast-Fourier-transformed (IFFT) images are reconstructed from mask-applied FFT of HRTEM images. The dislocations distinguished as lattice discontinuities are directly observed from these reconstructed IFFT images. The estimated dislocation density (N_D) is higher than 10^{12} cm^{-2}. The relatively low mobility measured in the hot-pressed In_4Se_{3-x} samples should result from the high density of dislocations and point defects. We believe that the increased grain-boundary density, dislocation density, nanoscale inclusions, and, especially, the Se vacant sites all contribute to the reduced phonon thermal conductivity κ_{ph}.

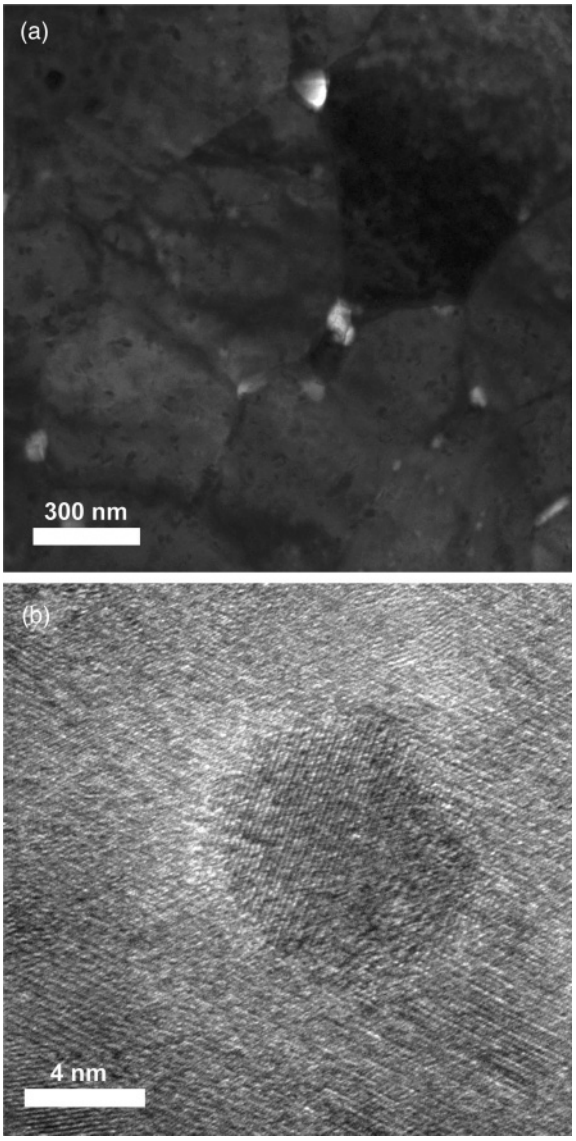

FIG. 3. (a) Low magnification TEM image of the typical hot-pressed In_4Se_{3-x} samples and (b) nanoscale inclusions found in high-resolution images.

A couple of interesting things need to be pointed out for this material system: (i) the electrical conductivity in the range of 2×10^2–6×10^3 Sm^{-1} is too low for the materials to be good thermoelectric materials with very high *ZT* so there is much room for improvement in *ZT* if a suitable dopant can be found to significantly increase the electrical conductivity without too much affecting the Seebeck coefficient, and (ii) the conducting behavior change from semiconducting to semimetallic with the Se deficiency deserves further detailed studies.

Dense bulk In_4Se_{3-x} samples with different Se deficiencies were prepared by ball milling and hot pressing. Semimetallic behavior was observed when the Se deficiency x is close to 0.5. High Se deficiency ($x = 0.65$ and 0.8) does not

deteriorate the electrical properties, but rather reduces the thermal conductivity, resulting in improved *ZT* values. A peak *ZT* of about 1 is achieved in $In_4Se_{2.2}$ at 425 °C, which is about 50% higher than the previously reported highest value for polycrystalline samples. This *ZT* enhancement mainly comes from the reduction of thermal conductivity due to the increased phonon scattering by high Se deficiency, defects, and nanoscale inclusions.

ACKNOWLEDGMENTS

The work was funded by the US Department of Energy under Contract No. DOE DE-FG02-00ER45805 (Z.F.R.), and Solid State Solar-Thermal Energy Conversion Center (S^3TEC), an Energy Frontier Research Center funded by the US Department of Energy, Office of Science, Office of Basic Energy Sciences, under Award No. DE-SC0001299 (G.C. and Z.F.R.).

*gchen2@mit.edu
†renzh@bc.edu

[1] C. Wood, Rep. Prog. Phys. **51**, 459 (1988).
[2] J. Rhyee, K. H. Lee, S. M. Lee, E. Cho, S. I. Kim, E. Lee, Y. S. Kwon, J. H. Shim, and G. Kotliar, Nature (London) **459**, 965 (2009).
[3] Y. B. Losovyj, M. Klinke, E. Cai, I. Rodriguez, J. Zhang, L. Makinistian, A. G. Petukhov, E. A. Albanesi, P. Galiy, Y. Fiyala, J. Liu, and P. A. Dowben, Appl. Phys. Lett. **92**, 122107 (2008).
[4] J. Rhyee, E. Cho, K. H. Lee, S. M. Lee, S. I. Kim, H. Kim, Y. S. Kwon, and S. J. Kim, Appl. Phys. Lett. **95**, 212106 (2009).
[5] X. Shi, J. Y. Cho, J. R. Salvador, J. Yang, and H. Wang, Appl. Phys. Lett. **96**, 162108 (2010).
[6] K. F. Hsu, S. Loo, F. Guo, W. Chen, J. S. Dyck, C. Uher, T. Hogan, E. K. Polychroniadis, and M. G. Kanatzidis, Science **303**, 818 (2004).
[7] B. Poudel, Q. Hao, Y. Ma, Y. C. Lan, A. Minnich, B. Yu, X. Yan, D. Z. Wang, A. Muto, D. Vashaee, X. Chen, J. M. Liu, M. S. Dresselhaus, G. Chen, and Z. F. Ren, Science **320**, 634 (2008).
[8] Yi Ma, Qing Hao, Bed Poudel, Yucheng Lan, Bo Yu, Dezhi Wang, Gang Chen, and Z. F. Ren, Nano Lett. **8**, 2580 (2008).
[9] G. Joshi, H. Lee, Y. C. Lan, X. W. Wang, G. H. Zhu, D. Z. Wang, A. J. Muto, M. Y. Tang, M. S. Dresselhaus, G. Chen, and Z. F. Ren, Nano Lett. **8**, 4670 (2008).
[10] X. W. Wang, H. Lee, Y. C. Lan, G. H. Zhu, G. Joshi, D. Z. Wang, J. Yang, A. J. Muto, M. Y. Tang, J. Klatsky, S. Song, M. S. Dresselhaus, G. Chen, and Z. F. Ren, Appl. Phys. Lett. **93**, 193121 (2008).
[11] G. H. Zhu, H. Lee, Y. C. Lan, X. W. Wang, G. Joshi, D. Z. Wang, J. Yang, D. Vashaee, H. Guilbert, A. Pillitteri, M. S. Dresselhaus, G. Chen, and Z. F. Ren, Phys. Rev. Lett. **102**, 196803 (2009).
[12] G. Chen, Semicond. Semimet. **71**, 203 (2001).
[13] M. S. Dresselhaus, G. Chen, Z. F. Ren, J. P. Fleurial, and P. Gogna, Adv. Mater. **19**, 1043 (2007).
[14] A. Majumdar, Science **303**, 777 (2004).
[15] H. Okamoto, J. Phase Equilibria Diffus. **25**, 201 (2004).
[16] C. Wood, A. Lockwood, A. Chmielewski, J. Parker, and A. Zoltan, Rev. Sci. Instrum. **55**, 110 (1984).